USE OF A MEMBRANE-BOUND FLUOROPHORE TO CHARACTERIZE DIFFUSION BOUNDARY LAYERS AROUND HUMAN ERYTHROCYTES

JULIE B. WILLIAMS* AND HOWARD KUTCHAI‡
*Departments of *Chemical Engineering and ‡Physiology, and ‡Biophysics Program, University of Virginia, Charlottesville, Virginia 22903*

ABSTRACT A novel method is used to demonstrate the presence of diffusion boundary layers around erythrocytes following rapid mixing in a stopped-flow spectrophotometer and to estimate the apparent dimensions of the diffusion boundary layers. Pink erythrocyte ghosts labeled on their external surfaces with tetramethyl rhodamine isothiocyanate (TRITC) were mixed in a stopped-flow apparatus with 50 mM NaI in Ringer's solutions. I^- is an effective collisional quencher of TRITC fluorescence. TRITC fluorescence after flow stopped decreased monoexponentially with time. The concentration of I^- at the cell surface as a function of time was estimated from the dependence of TRITC fluorescence on I^- concentration in steady-state experiments. The kinetics of the increase in I^- concentration at the cell surface was fit to two diffusional models: a planar erythrocyte ghost bounded by planar diffusion boundary layer and a spherical erythrocyte surrounded by a spherical shell diffusion boundary layer. The planar model best fits the experimental data with a diffusion boundary layer 4.68 μm thick. Using the spherical model the experimental data is best fit by a 6.9 μm diffusion boundary layer.

INTRODUCTION

A good deal of evidence suggests that immediately following the rapid mixing of erythrocytes by turbulent flow there exists around the erythrocytes a diffusion boundary layer (DBL) or unstirred layer. Estimates of the effective thickness of the DBL for oxygen uptake range from 1.5 μm (Coin and Olson, 1979) to 8 μm (Vandegriff and Olson, 1984). The DBL can be the major barrier to the uptake of oxygen by erythrocytes (Coin and Olson, 1979; Huxley and Kutchai, 1981; Weingarden et al., 1982)

Several investigators have estimated the thickness of the DBL around the red blood cell in rapid reaction devices. In view of the differences in the methods and apparatus employed, the estimates of effective DBL thickness are rather consistent. Sháafi et al. (1967) used the time delay in shrinking when red cells were mixed in a stopped-flow device with an hypertonic solution to estimate a DBL thickness of 5.5 μm. Coin and Olson (1979) fit their data on the kinetics of oxygen uptake by human erythrocytes with a planar model in which the thickness of the DBL was ~1.6 μm when flow stopped and then increased with time to ~3 μm. Huxley and Kutchai (1981) fit their oxygen uptake data to a planar model to estimate that the DBL after flow stopped was ~2 μm. Weingarden et al. (1982), using a planar model, found that an effective DBL 0.5 to 0.65 μm thick, could fit oxygen uptake data given by Roughton (1959). Kagawa and Mochizuki (1982) used a cylindrical model of the erythrocyte and its boundary layer to estimate an effective DBL thickness of ~4 μm for oxygen uptake. Brahm (1983), using a continuous flow device to study the uptake of alcohols, estimated an effective DBL thickness of <2 μm. Vandegriff and Olson (1984) fit oxygen uptake data to planar, spherical, and cylindrical models of the erythrocyte. In each case they found evidence that the effective thickness of the DBL is smallest just after flow stops and grows with time after that. They argue that the cylindrical model, which gives an effective DBL thickness of 3 to 8 μm, is most relevant to the real shape of red cells.

Several theoretical treatments yield estimates of effective DBL thickness around red blood cells in flow (see Rice, 1980; Huxley and Kutchai, 1983; and Vandegriff and Olson, 1984 for reviews). Friedlander (1957, 1961) and Harriott (1962) treated mass transfer to spherical particles in laminar flow. For particles the size and density of human red cell the equations of Harriott and Friedlander both reduce to $k = D/r$, where k is the minimum mass transfer coefficient, D is the diffusion coefficient and r is the radius of the particle. Taking D for iodide as 1.53×10^{-5} cm^2/s and $r = 3.3$ μm gives an estimate of the minimum mass transfer coefficient of 0.0463 cm/s. Taking the mass transfer coefficient to be equal to D/δ (where δ is the DBL thickness), gives an estimate of 3.3 μm for the effective DBL thickness. This is in reasonable agreement with experimental estimates of DBL thickness. Rice (1980) used the hydrodynamic theory of turbulent flow (Levich, 1962) to estimate that the effective DBL around a

human erythrocyte in turbulent flow should be of the order of 1 μm and should grow with time after flow stops. Using the value estimated by Gad-el-Hak et al. (1977) for the Kolmogoroff scale of red cells in turbulent flow, Vandegriff and Olson (1984) compute an estimate of 4 μm for the effective thickness of the DBL around a spherical red cell.

This paper describes the application of a novel method of demonstrating the existence of the DBL around erythrocytes and of estimating its effective thickness. Pink erythrocytes ghosts were prepared and the ghosts were labeled on their external surfaces with tetramethyl rhodamine isothiocyanate (TRITC). After TRITC-labeled pink ghosts were mixed rapidly in a stopped-flow device with an isotonic solution containing iodide, which quenches TRITC fluorescence, the fluorescence of TRITC declined exponentially. The time course of the decrease in TRITC fluorescence was used to estimate the concentration of iodide at the surface of the ghost as a function of time. The red cell ghost was modeled as a sphere and the DBL as a spherical shell surrounding the ghost. Comparison of the analytical solution of the diffusion equation for iodide in the spherical shell with the experimentally estimated concentration at the ghost surface as a function of time permitted an estimate of the effective thickness of the DBL.

MATERIALS AND METHODS

Materials

Tetramethyl rhodamine isothiocyanate (TRITC) was purchased from Research Organics, Inc. (Cleveland, OH) and bovine serum albumin from Sigma Chemical Co. (St. Louis, MO). Other chemicals used were reagent grade and were purchased from Sigma, Mallinckrodt Inc. (St. Louis, MO), or J. T. Baker (Phillipsburg, NJ) chemical companies.

Labeling Erythrocytes with TRITC

Freshly drawn human blood was centrifuged and erythrocytes were washed three times in phosphate-buffered saline. The buffy coat was removed with a Pasteur pipette. About 2 mg of TRITC was mixed with 250 ml of tris-buffered Ringer's solution, pH 8 (50 mM tris, pH 8; 132 mM NaCl; 1.9 mM KCl; 0.8 mM $CaCl_2$; and 0.47 mM $MgCl_2$), stirred for 60 min, and then centrifuged to remove any undissolved TRITC. Packed erythrocytes (1 ml) were added to 15 ml of TRITC solution and the mixture was stirred for 2 h at room temperature. Then 3 ml of 1% BSA in tris-buffered Ringer's solution, pH 8, was added and the labeled red cells centrifuged. The erythrocytes were washed in tris-buffered Ringer's solution (pH 7.4) until fluorescence of the supernatant was negligible.

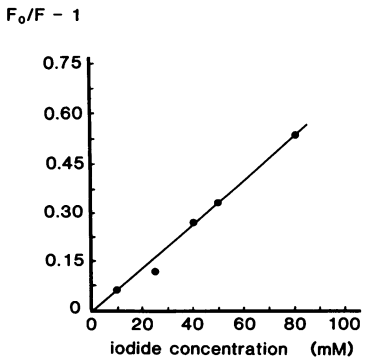

FIGURE 1 Stern-Volmer plot of the steady-state quenching of TRITC-labeled erythrocyte ghosts in the stopped-flow spectrophotometer. F_0 is the fluorescence intensity in absence of iodide, F is the fluorescence intensity in the presence of iodide.

Formation of Pink Erythrocyte Ghosts

Pink erythrocyte ghosts were prepared by the method of Steck (1974). Packed TRITC-labeled cells (1 ml) were added with rapid stirring to 500 mls of Steck's 5P8-1 Mg solution (5 mM phosphate, pH 8, with 1 mM $MgSO_4$). The ghosts were collected by centrifugation at 22,000 g for 10 min and washed four times in tris-buffered Ringer's solution, pH 7.4.

Kinetics of Quenching of TRITC Fluorescence

TRITC-labeled pink erythrocyte ghosts at a hematocrit of 1% were rapidly mixed with 50 mM NaI in tris-buffered Ringer's solution using a Durrum-Gibson Model D-110 stopped-flow spectrophotometer (Dionex Corp., Sunnyvale, CA) equipped with a fluorescence cuvette. TRITC was excited using light from a 250 W quartz halogen lamp (Osram) passed through a 546 nm interference filter. Emitted light was collected at 580 nm using an interference filter and an end-on photomultiplier tube (model R562HA; Hamamatsu Corp., Middleton, NJ). The amplified output of the photomultiplier tube was collected by a North Star Horizon II microcomputer using the software developed by On-line Instrument Systems (Jefferson, GA).

RESULTS

Steady-state Quenching of Fluorescence of TRITC-labeled Ghosts by Iodide

Steady-state quenching of fluorescence of TRITC-labeled pink ghosts was studied by mixing labeled ghosts with different concentrations of NaI in the stopped-flow apparatus and recording the steady-state level of fluorescence that resulted. Fig. 1 shows the data from such an experiment displayed on a Stern-Volmer Plot. The linearity of the Stern-Volmer Plot is consistent with the interpretations that the quenching by I^- of TRITC fluorescence is purely collisional and that there is no significant pool of TRITC that is unavailable to the quencher. In the range of I^- concentrations employed in further studies (0 to 50 mM), the fluorescence of TRITC-labeled ghosts is nearly inversely proportional to I^- concentration.

Kinetics of Quenching of Fluorescence of TRITC-labeled Ghosts by Iodide

When TRITC-labeled ghosts (1% hematocrit) were mixed with 50 mM NaI in the stopped-flow apparatus and the fluorescence of TRITC followed in time, results like those in Fig. 2 were obtained. Mixing the ghosts with tris-buffered Ringer's solution, pH 7.4, gave a tracing with noise, but no average change in fluorescence with time. To a first approximation the decrease in TRITC fluorescence was mono-exponential in time. The apparent first-order rate constant obtained in the experiment of Fig. 2 (the

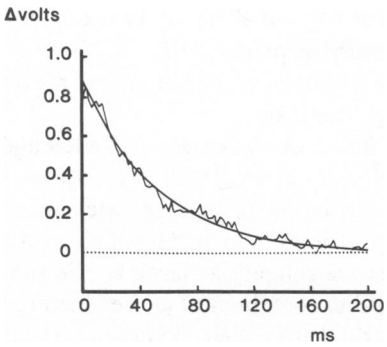

FIGURE 2 The kinetics of quenching by iodide of the fluorescence of TRITC-labeled erythrocyte ghosts. TRITC-labeled ghosts at 1% hematocrit were mixed with 50 mM NaI in Ringer's solution and fluorescence was followed as a function of time. The ordinate gives fluorescence intensity, in volts, relative to the steady-state fluorescence intensity. The tracing shown is the average of 10 individual records.

average of 10 runs in the stopped flow) is 18.8 s^{-1}. The entire experiment (TRITC-labeling, ghost preparation, stopped-flow runs) was repeated three times with similar results and rate constants of 16.4, 17.7, and 17.7 s^{-1}. The average rate constant is 17.65 ± 0.85 s^{-1}. This corresponds to an average half-time for quenching of 39.3 ms. The results were not altered by the presence of 40 μM DIDS (4,4′-diisothiocyano-2,2′-disulfonic acid stilbene), a potent inhibitor of transport of iodide across the erythrocyte membrane, suggesting we are not observing quenching by I^- of TRITC located inside the labeled ghosts. On the average, 5% of the TRITC-labeled ghosts were hemolyzed by passage through the stopped-flow mixing device.

ANALYSIS OF RESULTS

Estimation of the Effective Thickness of the DBL

Mathematical models of the TRITC-labeled erythrocyte ghosts and its surrounding DBL were used to estimate the effective thickness of the DBL. Both a plane sheet model and a spherical model were used. Tosteson (1959) found that I^- exchanges for Cl^- across the membrane of the human erythrocyte with a half-time of 9.9 s. We thus assumed that I^- does not permeate the membrane of the TRITC-labeled ghosts on the time scale of our measurements. Our finding that 40 μM DIDS had no effect on the kinetics of quenching supports this assumption.

Planar Model

Fig. 3 *A* schematically depicts the planar model of the TRITC-labeled erythrocyte ghost with its DBL. The erythrocyte ghost and its surrounding DBLs are modeled as infinite layers. The erythrocyte membrane is assumed to be impermeable to I^- on the time scale of our measurements. The relevant diffusion equation for I^- in the DBL is

$$\partial C/\partial t = D\,\partial^2 C/\partial x^2, \quad (1)$$

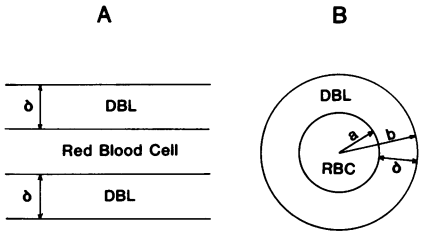

FIGURE 3 Models of the erythrocyte and its surrounding diffusion boundary layers. (*A*) A planar model in which the erythrocyte and the DBL are modeled as infinite layers. (*B*) A spherical model.

where D is the diffusion coefficient, C is the iodide concentration, t is time and x is position normal to the plane of the layers. We take the position of the surface of the red cell to be $x = 0$ and the thickness of the DBL to be δ. In the well-mixed Ringer's solution outside the DBL the concentration of I^- is C_o. Our assumption that the cell membrane of the red cell ghost is impermeable to I^- on the time scale of our measurements leads to the boundary condition that

$$\text{at } x = 0,\ \partial C/\partial x = 0 \text{ for } t \geq 0. \quad (2)$$

The solution (Hill, 1965) is

$$C/C_o = 1 - (4/\pi)\sum_{n=0}^{n=\infty}[(-1)^n/(2n+1)]e^{-\alpha} \cdot (2n+1)^2\, t \cos[(2n+1)\pi x/(2\delta)], \quad (3)$$

where $\alpha = D\pi^2/4\delta^2)$. The series converges rapidly for values of $\alpha t > 1$, the sum of all the terms after the first is <0.0001 (Hill, 1965). Assuming that $D = 1.5 \times 10^{-5}$ cm^2/s and $\delta = 5 \times 10^{-4}$ cm, we compute a value of $\alpha = 148$ s^{-1}. Thus for $t > 6.75$ ms, only the first term of the series need be considered. At the surface of the erythrocyte ghost (at $x = 0$), taking only the first term of Eq. 3, we obtain

$$C/C_o = 1 - (4/\pi)e^{-\alpha t}. \quad (4)$$

We then proceeded to fit Eq. 4 to our experimental results as follows. The Stern-Volmer Equation, with the value of the quenching constant as determined in the experiments shown in Fig. 1, was used to convert our experimental values of fluorescence after mixing to values of iodide concentration at the surface of the erythrocyte ghosts. The iodide concentration at the ghost surface was found to exponentially approach the concentration of I^- in the medium (50 mM) with a rate constant that averaged 0.171 s^{-1}. Equating Eq. 4 with our experimentally-derived equations for $[I^-]$ at the ghost surface

$$C = C_o(1 - e^{-kt}) \quad (5)$$

gives

$$\alpha = -(1/t)\ln[(\pi/4)e^{-kt}]. \quad (6)$$

Using $k = 0.171$ s^{-1} values of α were computed. The values of α converge rapidly to 0.172 as time increases. Taking the

diffusion coefficient for I^- to be 1.53×10^{-5} cm^2/s (Robinson and Stokes, 1959), we compute a value for δ of 4.68 μm.

Spherical Model

Fig. 3 *B* schematically depicts the spherical model of the erythrocyte ghost and the surrounding DBL. The diffusion equation that applies in the DBL is

$$\partial C/\partial t = (D/r^2)\partial/\partial r(r^2\partial C/\partial r), \quad (7)$$

with the following initial values and boundary conditions:

$$\begin{aligned} &\text{at } t = 0, \quad C = 0 \text{ for } a \le r \le b \\ &\text{at } r = b, \quad C = C_0 \text{ for } t > 0 \\ &\text{at } r = a, \quad \partial C/\partial r = 0 \text{ for } t \ge 0. \end{aligned} \quad (8)$$

To solve Eq. 7 subject to the constraints of Eq. 8, dimensionless variables were introduced and the method of separation of variables was used to obtain the solution

$$C = C_0 + (1/r)\sum_{n=1}^{\infty} A_n e^{-\lambda_n^2 Dt} \cdot \{\sin[\lambda_n(r-a)] + a\lambda_n \cos[\lambda_n(r-a)]\}, \quad (9)$$

where the eigenvalues (λ_n) are defined by

$$\tan[\lambda_n(b-a)] = -\lambda_n a. \quad (10)$$

At the surface of the erythrocyte ghost (at $r = a$) the solution (Eq. 9) becomes

$$C = C_0 + \sum_{n=1}^{\infty} A_n \lambda_n e^{-\lambda_n^2 Dt}. \quad (11)$$

If a is taken to be 3.3 μm (the radius of a sphere with surface area equal to that of a human red cell) and b is allowed to vary from 1.65 μm to 13.2 μm ($a/2$ to $4a$), Eq. 10 converges sufficiently rapidly that the error caused by using only the first term in the series is negligible. Thus the spherical model predicts that the concentration of I^- at the surface of the ghost will approach the $[I^-]$ in the medium monoexponentially in agreement with our experimental results. Our experimental data fit an exponential approach of $[I^-]$ at the ghost surface to $[I^-]$ in the medium with an apparent rate constant of 0.171 s^{-1}. The spherical model predicts an apparent rate constant of $(-\lambda_1 D)$. Setting the two rate constants equal and solving for λ_1 gives $\lambda_1 = 3.34 \times 10^{-1}$. Substituting this value of λ_1 into Eq. 10 allows calculation of an apparent DBL thickness ($\delta = b - a$) of 6.9 μm.

DISCUSSION

Our experimental data on the kinetics of quenching of TRITC on the surface of erythrocyte ghosts are fit by a model of a spherical cell surrounded by a spherical shell boundary layer 6.9 μm thick or by a model of a planar erythrocyte with a planar DBL 4.7 μm thick. These estimates are within the range of values previously determined by other methods.

Turbulent flow is characterized by eddies and quasilaminar flow regions (Levich, 1962; Rice, 1980). The eddies have a wide distribution of sizes and are in random motion relative to one another. In turbulent flow in a tube, the largest eddies are roughly as large as the tube diameter. The largest eddies contain most of the kinetic energy of the turbulence and transfer their momentum to intermediate-sized eddies. The intermediate-sized eddies transfer their momentum to still smaller eddies, and so forth. In the smallest eddies in the flow viscous damping is the main means of dissipating the kinetic energy of the flow. For the dimensions and flow rates that are employed in typical rapid reaction devices, the smallest eddies present in turbulent flow are ~50 μm across (Gad-el-Hak et al., 1977). Thus, at any instant, a red blood cell in a turbulent flow would find itself embedded in a quasilaminar eddy much larger than the cell itself. Just at the surface of the red cell the velocity of fluid flow, relative to the cell, is zero. Thus in some region around the cell the transfer of mass by convection is very slow relative to mass transfer by diffusion. This region is called the diffusion boundary layer (DBL). When a red cell in turbulent flow is taking up a solute the concentration of that solute will vary with position within the DBL.

It should be emphasized that the DBL is not a static layer. Within the DBL diffusion is the predominant mechanism of mass transfer, but at greater distances from the cell the contribution of convective mass transfer increases. At some distance from the cell convective transfer will exceed transfer due to diffusion. Thus the boundary of the DBL is not clearly defined. The greater the distance from the cell, the greater the convective mixing, so that at some distance the concentration of solute ceases to vary appreciably with position. The most common definition of DBL, as that region in which concentration varies with position, makes sense in these terms. Since the eddies in the flow are in random motion relative to one another, the thickness of the DBL around each red cell will vary in time and space. The experimentally determined DBL thickness must be regarded as an estimate of the time average for a large number of red cells.

Statistical theories of turbulence (Levich, 1962) permit order-of-magnitude estimates of DBL thickness in turbulent flow. In stopped-flow experiments these estimates should apply most closely to the time just before flow stops. After flow stops turbulence decays in time, becomes quasilaminar, and finally flow ceases. For aqueous solutions under the conditions commonly employed in rapid kinetic studies, turbulence decays with a time constant of the order of 10 ms (Rice, 1980). After turbulence has decayed to quasilaminar flow, other estimates of effective DBL thickness apply (Friedlander, 1957, 1961; Harriott, 1962).

Consider a red blood cell after flow stops. It is embedded in a DBL in which mass transfer is principally by diffusion and convective mass transfer is negligible. As turbulence decays the size of the region around the cell in which mass transfer by convection is negligible will increase, so that the effective thickness of the DBL will increase in time. For a solute that is taken up by the cell, each red cell will tend to deplete the solution around it of the transported solute. This will tend to further expand the region around the cell in which concentration varies with position. For a solute taken up by the cell the DBL grows with time after flow stops due to both of these mechanisms, decay of turbulence and solute uptake by the cell. Thus theoretical estimates of the kinetics of growth of the DBL due to hydrodynamic factors alone should underestimate the rate of growth of the DBL for a solute that is taken up by the cell. Using an effectively impermeant solute to estimate the effective thickness of the DBL has the advantage that growth of the DBL after flow stops will be due only to hydrodynamic factors.

Coin and Olson (1979) provided experimental support for the growth of the DBL after flow stops. Their data could only be fit by a planar model in which the thickness of the DBL increased with time. Vandegriff and Olson (1984) found that when a disc-shaped model is used, a constant DBL thickness of 8 μm fits their oxygen uptake data reasonably well, although their data conform better with the interpretation that the DBL is 1 μm thick immediately after flow stops and then grows with time.

In oxygen uptake experiments the continuing uptake of oxygen by the red cells presumably contributes to the growth of the DBL after flow stops. In the experiments presented here, since iodide does not enter the cells during the time course of our measurements, the depletion of iodide by the cells does not contribute to the growth of the DBL with time. In previous oxygen uptake studies in this laboratory Huxley and Kutchai, 1981) it was found that the rate of oxygen uptake was initially first-order in time, but at later times deviated from first-order kinetics in a manner consistent with a growth of the DBL after flow stops. However, in the present studies the entire time course of iodide diffusion to the erythrocyte ghost surface could be fit reasonably well (correlation coefficient >0.9) by a single first-order rate constant. The mechanisms by which the effective DBL around erythrocytes grows after flow stops deserve further inquiry.

Summary

We report here the use of a novel method to demonstrate the existence and estimate the effective size of the DBL around erythrocytes. Most of the previous estimates of the effective thickness of the DBL around erythrocytes depend on quantitative comparison of the rate of oxygen uptake observed with rates calculated from mathematical models that include the influence of a DBL. The method reported here has the advantage of giving a qualitative indication of the presence of the DBL, namely the time dependence of quenching of the fluorophore after mixing. A second advantage of the fluorescence quenching method for probing the DBL is that the simplification that results from assuming that the plasma membrane is impermeable to iodide allows analytical solution of the diffusion equations for certain geometries. Another simplification that results from the lack of permeation of the cell by iodide during the measurement is that the DBL does not grow due to iodide uptake after flow stops. The DBL should still grow after the flow stops due to hydrodynamic factors. The fluorescence quenching method may be useful in more detailed experimental characterization of the growth of the diffusion boundary layer after flow stops due to hydrodynamic factors.

This research was supported by grant HL30900 from the National Heart, Lung, and Blood Institute.

The research presented here was part of the thesis submitted by Julie B. Williams for the M.S. degree in Chemical Engineering from the University of Virginia. Helpful discussions with Dr. Donald J. Kirwan are gratefully acknowledged.

Received for publication 16 May 1985 and in final form 14 August 1985.

REFERENCES

Brahm, J. 1983. Permeability of human red cells to a homologous series of aliphatic alcohols. *J. Gen. Physiol.* 81:283–304.

Coin, J. T., and J. S. Olson. 1979. Rate of oxygen uptake by human red blood cells. *J. Biol. Chem.* 254:1178–1190.

Friedlander, S. K. 1957. Heat and mass transfer to single spheres and cylinders at low Reynolds number. *Am. Inst. Chem. Eng. J.* 3:43–48.

Friedlander, S. K. 1961. A note on transport to spheres in Stokes flow. *Am. Inst. Chem. Eng. J.* 7:347–348.

Gad-el-Hak, M., J. B. Morton, and H. Kutchai. 1977. Turbulent flow of red cells in dilute suspensions. Effects on kinetics of oxygen uptake. *Biophys. J.* 18:298–300.

Harriott, P. 1962. Mass transfer to particles: Part I. Suspended in agitated tanks. *Am. Inst. Chem. Eng. J.* 8:93–95.

Hill, A. V. 1965. Trails and trials in physiology. Williams and Wilkins, Baltimore. 223.

Huxley, V. H., and H. Kutchai. 1981. The effect of the red cell membrane and a diffusion boundary layer on the rate of oxygen uptake by human erythrocytes. *J. Physiol. (Lond.)*. 75–83.

Huxley, V. H., and H. Kutchai. 1983. Effects of diffusion boundary layers on the initial uptake of oxygen by red blood cells. Theory vs. experiment. *Microvasc. Res.* 26:89–107.

Kagawa, T., and M. Mochizuki. 1982. Numerical solution of partial differential equation describing oxygenation rate of the red blood cell. *Jpn. J. Physiol.* 32:197–218.

Lakowicz, J. R. 1983. Principles of fluorescence spectroscopy. Plenum Publishing Corp., New York. 260–264.

Levich, V. G. 1962. Physicochemical hydrodynamics. Prentice-Hall, Englewood, NJ. 700 pp.

Rice, S. A. 1980. Hydrodynamic and diffusional considerations of rapid-mix experiments with red blood cells. *Biophys. J.* 29:65–77.

Robinson, R. A., and R. H. Stokes. 1959. Electrolyte solutions. Butterworth Scientific Publications, New York. 559 pp.

Roughton, F. J. W. 1959. Diffusion and simultaneous reaction velocity as joint factors in determining the rate of uptake of oxygen and carbon

monoxide by the red blood corpuscle. *Progr. Biophys. Biophys. Chem.* 9:56–104.

Sháafi, R. I., G. I. Rich, V. N. Sidel, W. Bossert, and A. K. Solomon. 1967. The effect of unstirred layers on human red cell water permeability. *J. Gen. Physiol.* 50:1377–1399.

Steck, T. L., and J. A. Kant. 1974. Preparation of impermeable ghosts and inside-out vesicles from human erythrocyte membranes. *Methods Enzymol.* 31:172–180.

Tosteson, D. C. 1959. Halide transport in red blood cells. *Acta Physiol. Scand.* 46:19–41.

Vandegriff, K. D., and J. S. Olson. 1984. A quantitative description in three dimensions of oxygen uptake by human red blood cells. *Biophys. J.* 45:825–835.

Weingarden, M., H. Mizukami, and S. A. Rice. 1982. Factors defining the rate of oxygen uptake by the red blood cell. *Bull. Math. Biol.* 44:135–147.